

2-11-2021

Forced Convection from Heat Source on A Conductive Plate in an Air Rectangular Channel.

F. Araid

Mechanical Power Engineering Department., Faculty of Engineering., El-Mansoura University., Mansoura., Egypt.

Follow this and additional works at: <https://mej.researchcommons.org/home>

Recommended Citation

Araid, F. (2021) "Forced Convection from Heat Source on A Conductive Plate in an Air Rectangular Channel.," *Mansoura Engineering Journal*: Vol. 24 : Iss. 2 , Article 12.

Available at: <https://doi.org/10.21608/bfemu.2021.147887>

This Original Study is brought to you for free and open access by Mansoura Engineering Journal. It has been accepted for inclusion in Mansoura Engineering Journal by an authorized editor of Mansoura Engineering Journal. For more information, please contact mej@mans.edu.eg.

FORCED CONVECTION FROM HEAT SOURCE ON A CONDUCTIVE PLATE IN AN AIR RECTANGULAR CHANNEL

الحمل الجبرى لمصدر حرارى على سطح موصل فى مجرى هوائى مستطيل

F. F. Araid

Mechanical Power Engineering Department
Mansoura University, Egypt

خلاصة:

يقدم هذا البحث دراسة تجريبية لانتقال الحرارة بالحمل الجبرى من مصدر حرارى مثبت على قاعدة معدنية فى مجرى هوائى مستطيل أفقى، والمصدر الحرارى مكون من قطاع المنيوم مستطيل الشكل مصقول ابعاده الخارجية 27 مم عرض و 16 مم ارتفاع و 120 مم طول و 1 مم سمك ، ومثبت بداخله سخان كهربى من النيكل كروم ملفوف حول قلب من السيراميك ومثبت فى منتصف قاعدة من الالمنيوم سمكها 1 مم وطولها 135 مم وعرضها 20 مم، يقاس توزيع درجات الحرارة على أوجه المصدر الحرارى والسطح المعدنى بأزواج حرارية من النحاس والكونستنتان بقطر 0.3 مم، وقد أجريت التجارب عند سرعات مختلفة بحيث تغير رقم رينولدز من 20600 الى 63700 بينما تغيرت القدرة الكهربائية للمصدر الحرارى من 6 وات الى 70 وات، وقد تم تصوير شكل السريان وتوزيعه على السطح المعدنى والمصدر الحرارى، واستنتج من الدراسة انه بتثبيت السطح المعدنى اسفل المنبع الحرارى لادى الى انتقال جزء من الحرارة المولدة فى المصدر الى هذا السطح مما ادى الى تخفيض درجة حرارة المصدر الحرارى الموضعية والمتوسطة ودرجة حرارته القصوى، ويتزايد معدل الانخفاض فى درجة الحرارة بزيادة رقم رينولدز، كما استنتجت معادلات لحساب درجة الحرارة القصوى للمصدر الحرارى وكذلك علاقات لابعدية بين رقم نوسيلت المتوسط ورقم رينولدز لحساب معامل انتقال الحرارة المتوسط بين المصدر الحرارى ذو القاعدة الموصلة وتيار الهواء.

ABSTRACT

Forced convection heat transfer from heat source attached to a conductive base plate in a horizontal rectangular channel is investigated experimentally. The heat source module is a highly polished aluminum parallelogram of 27mm wide, 16mm height and 120 mm long is fixed on a sheet of aluminum of 137 mm long, 120 mm wide and 1 mm thickness. The dependence of the heat flow characteristics on Reynolds number and the heat-generated in the heat source module were investigated for a range of Reynolds number 20500 to 63700, meanwhile the generated power from the heat source changes from 6W to 70 W. The conductive base plate absorbs heat from the heat source, which in turns decreases the level of the local heater surface temperature. Reynolds number has a great effect on the absorbed heat flux by the conductive plate from the heater and with the increase of Reynolds number, the local surface temperatures of the heater and base plate decrease. The maximum temperature and average Nusselt number along the five surfaces of the base plate and the heater is correlated with Reynolds number for fixed values of heat generation by power relations. Also, flow visualization is performed indicating the pattern of the flow path of air over the heater module.

INTRODUCTION

An area which has a considerable amount of research activity in the recent years is that of heat removal from electronic circuitry. Since the performance of electronic components is often strongly temperature dependent, there is a growing need to develop suitable methods for the cooling of electronic packages that are employed in a wide variety of applications, such as air space travel, communication and naval systems and computers. Air-cooling is still the most attractive method for computer systems and other electronic equipment, due to its simplicity and low cost. Thermal engineers in the electronics industry are always trying to achieve the best possible performance out of air-cooling. In this effort, the need for understanding the flow phenomena and convective heat transfer mechanisms that are present in air-cooled electronic systems is obvious.

Previously, many investigators studied the various modes of heat transfer and relevant configurations along with the associated heat transfer. Extensive surveys of literature in this field have been presented by Jaluria [1], Incropera [2], Papanicolaou and Jaluria [3] and El-Kady and Araid [4].

Among the work dealing with forced convection cooling of electronic equipment, is that of Ramadhyani et al. [5], the heat transfer from discrete heat sources mounted on one wall of a channel and exposed to fully developed laminar flow is studied theoretically. Incropera et al. [6], investigated experimentally the convection heat transfer from a single heat source and an in-line four rows array of 12 heat sources which are flush mounted on a wall of a horizontal rectangular channel. Davalath and Bayazitoglu [7] developed a model for numerical prediction of various flows and forced convection between parallel plates with finite block heat sources. Wadsworth and Mudawar [8], investigated heat transfer from smooth simulated chip to a two-dimensional jet of dielectric fluorinate FC-72 liquid issuing from a thin rectangular slot into a channel confined between the chip surface and nozzle plate. Kim and Anand [9] studied theoretically laminar developing flow and heat transfer between a series of parallel plates with surface mounted discrete heat sources. Kim and Anand [10], through a theoretical study, investigated the turbulent heat transfer between a series of parallel plates with surface mounted discrete heat sources using the $K-\epsilon$ model. Molki et al. [11], focused their work on the effect of entrance length on heat transfer coefficients and associated thermal wake effects. Their experimental data is used to correlate the heat transfer coefficient, entrance length and operating parameters. Hwang and Liou [12] studied the heat transfer and friction in a low aspect ratio rectangular channel with staggered perforated ribs on two opposite walls. They showed the effects of perforated rib open area ratio, rib pitch to height ratio, rib-height to channel hydraulic diameter ratio, rib alignment and Reynolds number on heat transfer and friction factor. Nakayama and Park [13], obtained experimentally and theoretically the conjugate heat transfer from a single surface mounted block to forced convection air flow in a channel. They have taken into account the effect of thermal wake shed from the block on the heat transfer from the floor of the test section. Fowler et al. [14], developed through experimental and numerical study, the optimum geometric arrangement of staggered parallel plates in a fixed volume with forced convection heat transfer rate.

These studies illustrate the lack of the experimental knowledge in forced convection from protruding heat sources, specially those attached on conductive base plate, which is the more realistic thermal condition. The present study is directed to investigate experimentally the heat transfer characteristics due to the forced convection from one protruding heat source attached to a conductive base-plate in a

rectangular horizontal channel. The dependence of the heat flow characteristics on Reynolds number and the heat-generated in the heat source module are investigated. Correlations for the average Nusselt number and maximum heater surface temperature are developed as a function of Reynolds number for fixed values of the generated heat energy. Also, flow visualization is performed indicating the pattern of fluid flow adjacent to the heater and base plate surfaces.

EXPERIMENTAL WORK

The test-rig which is constructed for the planned experimental work, is shown in Fig. 1-a. It consists of a wind channel with 120x120 mm square cross section of wood and 1500 mm long. The air from the laboratory room is drawn through the system by a centrifugal fan (10), driven by one horsepower electric motor (12) and having its inlet connected to the working section. Air enters the apparatus by way of a bellmouth (2) and a fine mesh screen (1) to ensure a fairly uniform flow with negligible turbulence through the test section. After the working section a transition piece leads to the fan inlet and carries a honeycomb flow straightener (8) intended to prevent the transmission of swirl from the fan back into the working section. The fan discharges to a graduated throttle valve (13) by means of which the air velocity through the apparatus may be regulated. In between the main channel and the fan, flexible textile plastic connection (9) is fitted in order to eliminate any vibration transmission to the honeycomb section (8).

The air velocity is measured with the help of a Pitot-tube (5) and an inclined alcohol manometer (21) at the centers of nine imaginary equal areas into which the Pitot tube is situated 500 mm downstream. The air velocity is also measured by a hot wire probe (6) located at 750 mm downstream. The difference in velocity values measured by the two methods is less than $\pm 1.5\%$.

The heating element construction with its base plate is shown in Fig. 1-b. The heating element face is made of a Nickel-Chromium electric heater with rectangular cross section of 0.5x1.5 mm is wrapped at equal pitches over the sides of Bakelite core of 22 mm wide, 14 mm height and 120 mm long (26). This core is surrounded by mica sheets of 0.5mm thickness (27) and is inserted inside a highly polished aluminum channel of 27mm wide, 16mm height and 120 mm long (23). The heat source module is fixed on a sheet of aluminum of 135 mm long, 120 mm wide and 1mm thickness (24). The aluminum sheet is fixed on a sheet of mica of 0.5mm thickness (25) and then fixed on the wall of the channel, which is made of 20 mm thickness wood.

An auto transformer (17) is used to control the heat input to the heating element as well as one voltmeter (16) and an ammeter (15). The input power to the heating element was checked by using a Wattmeter (20) as shown in Fig. (1-b).

The heater surface temperature was measured by six copper-constantan thermocouples of 0.5-mm diameter and the temperature of the base plate was measured by 14 thermocouples from the same kind. The thermocouple distribution along the heater surfaces and the base plate is shown in Fig. (1-b). The thermocouples were connected to a 24-points Yokogawa digital temperature recorder of a sensitivity of 0.1°C (23).

During the course of the experimental work nearly two hours were needed to reach the steady state condition. This condition was satisfied when there were no change in the temperature reading within a time period of about 15 minutes.

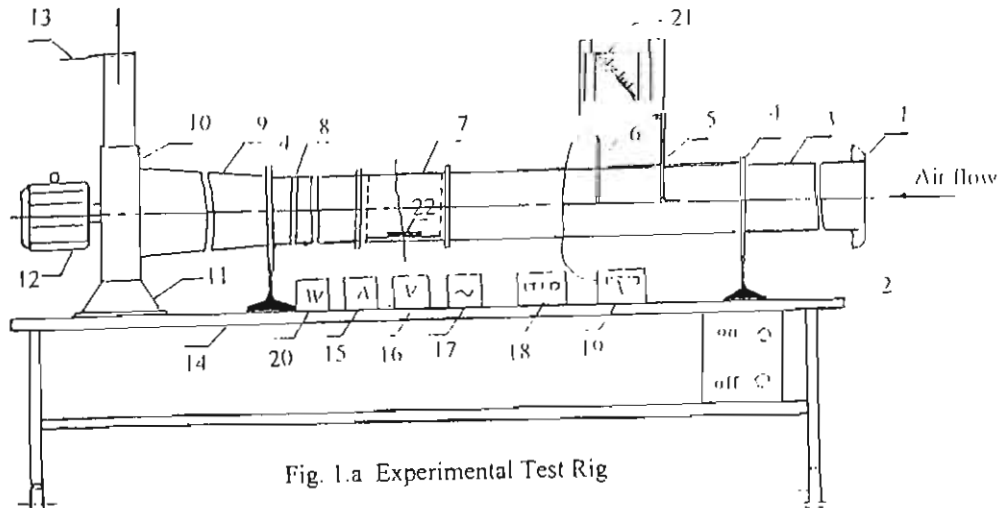


Fig. 1.a Experimental Test Rig

1- Fine mesh screen, 2- Bellmouth, 3- Straight channel, 4- Supports, 5- Pitot tube, 6- Hot wire anemometer probe, 7- Test section, 8- Honeycomb, 9- Flexible connection, 10- Downstream blower, 11- Blower supports, 12- Electric motor, 13- Discharge control gate, 14- Movable table, 15- Ammeter, 16- Voltmeter, 17- Auto transformer, 18- Temperature recorder, 19- Hot wire anemometer, 20- Wattmeter, 21- Inclined manometer, 22- Heating element.

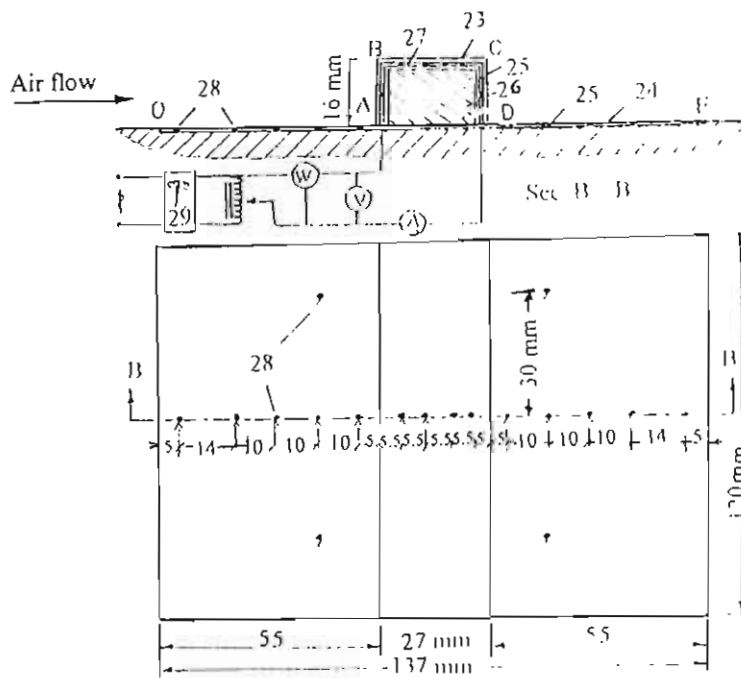


Fig. 1.b. Heating Element Construction With Its Base Plate

23- Aluminium channel, 24- Stainless-steel sheet, 25- Mica sheet, 26- Backalite core, 27- Nickel-Chromium electric heater, 28- Copper-constantan thermocouple, 29- Stabilizer

average heat transfer coefficient along the surface of the heater is presented in Figure 1. Due to the unique geometry of the experimental system, two different characteristic lengths have been used to correlate the heat transfer data. Since the hydrodynamics corresponds to internal channel flow, the hydraulic diameter is used in calculating the Reynolds number. However, since thermal boundary layer development is more closely associated with parallel flow over a plane surface, it is appropriate to base the Nusselt number on the heat source length [15]. Hence the Nusselt number and Reynolds number are defined as:

$$\bar{Nu} = (q L / k) / (\bar{T} - T_o)$$

$$Re = u_o D / \nu$$

Where, T_o , \bar{T} , k , u_o , D and ν are the air entering temperature and the average heater surface temperature, the thermal conductivity, air flow mean velocity, channel hydraulic diameter and fluid kinematic viscosity, respectively.

RESULTS AND DISCUSSION

Experimental results were obtained for the forced convection from a single protruding heat source, which is attached on the conductive plate. The range of airflow velocity is from 2.56 to 7.96 m/s, which gives range of Reynolds numbers from 20500 to 63700. The heat generated from the heat source was varied from 6 to 70 W. The effect of Reynolds number and the generated heat power from the heater on the local and maximum surface temperatures and the local and average Nusselt number were presented.

The main purpose of this work is to investigate the heat transfer characteristics by specifying more realistic thermal conditions. One of the main heat transfer characteristics is the local temperature and in turn the maximum temperature of the heat source face, which has the great influence on the design of the upstream and downstream parts of the base plate OA and DE and the heater three faces AB, B and CD for different values of Reynolds numbers; $Re = 20500, 33600, 58000$ and 63700 and four fixed values of generated power $Q = 6, 22, 51$ and $70W$. Figure 2 shows sudden decrease of the temperature at the base plate in the downstream regions adjacent to the heater vertical surfaces. In the rest of the plate the temperature decreases with very low rates with the increase of the distance from the heater. The temperature of the leading edge of the trailing edge is higher than the inlet flow temperature. Also, the temperature of the trailing edge of the base plate portion is much higher than the following adiabatic surface (point D). This means that, the base plate absorbs the heat from the heater and transfers it to the flowing air at its whole length. Also, it means that of the base plate length, it can absorb more heat from the heater than the maximum temperature occurs as expected at the right top surface (point D). With the increase of Reynolds number, the maximum temperature decreases.

The maximum temperature of the downstream and upstream surfaces of the heater OA and DE as well as the three surfaces of the heater AB, B and CD in Fig. 3 for Reynolds number $20500 \leq Re \leq 63700$

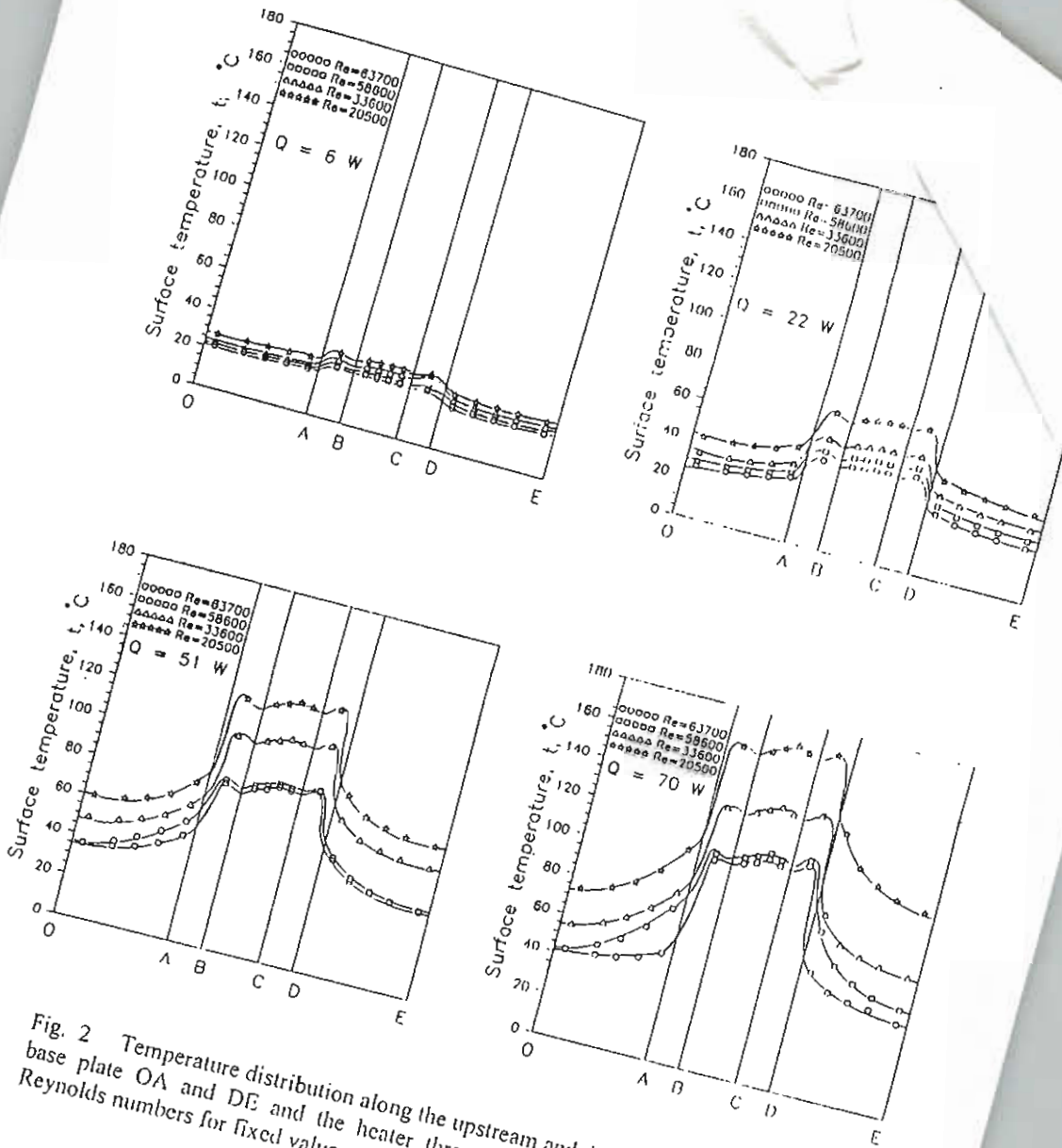


Fig. 2 Temperature distribution along the upstream and downstream parts of the base plate OA and DE and the heater three faces AB, BC, and CD at different Reynolds numbers for fixed values of heat input $Q=6, 22, 51$ and 70 W .

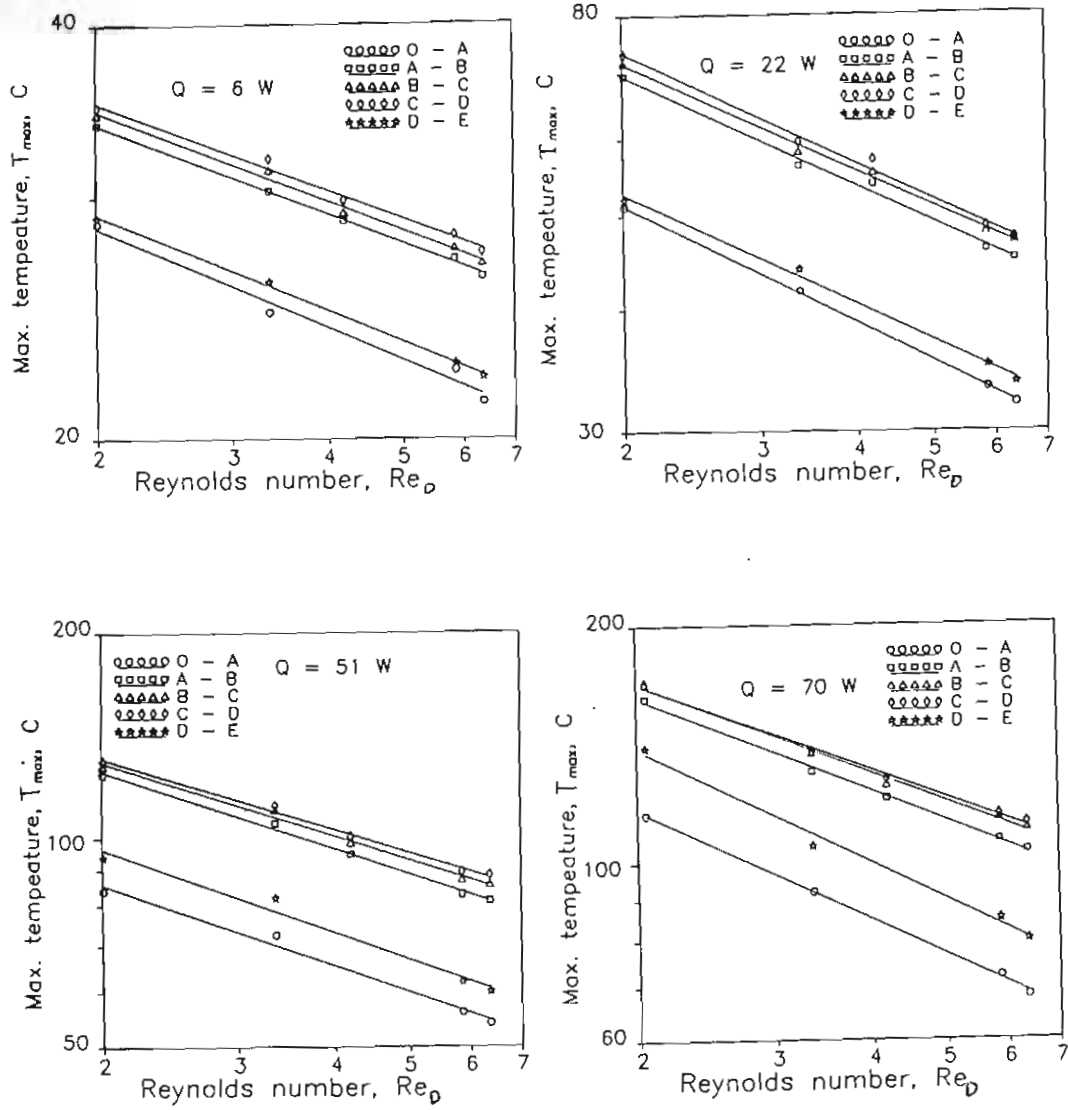


Fig. 3 Variation of maximum temperature of the downstream and upstream base plate sections OA and DE and the three surfaces of the heater AB, BC, and CD for Reynolds number $20500 \leq Re \leq 63000$ and fixed heating values of $Q=6, 22, 51$ and $70W$.

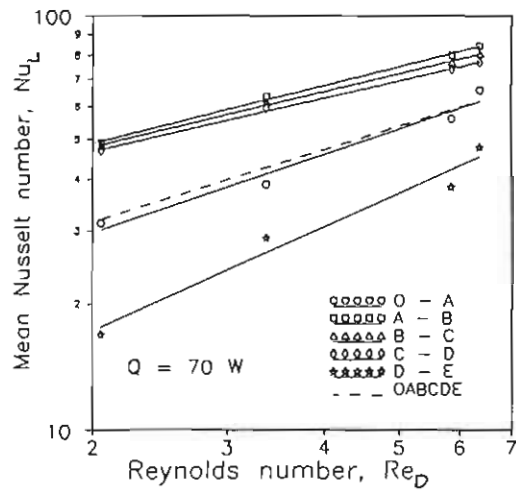
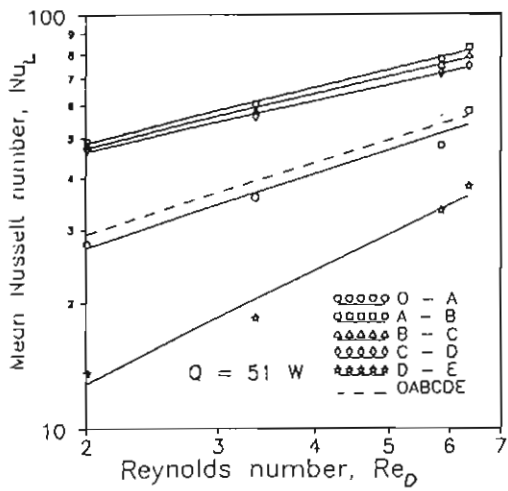
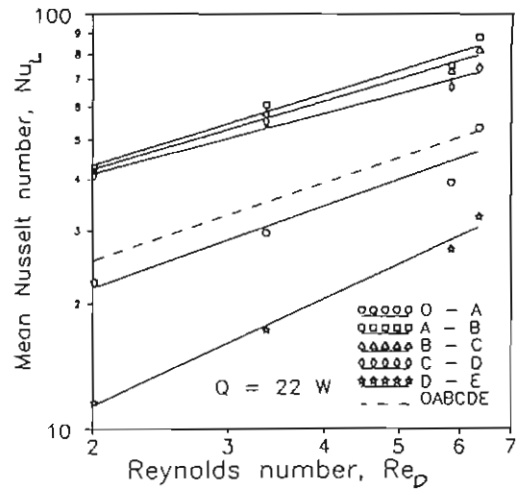
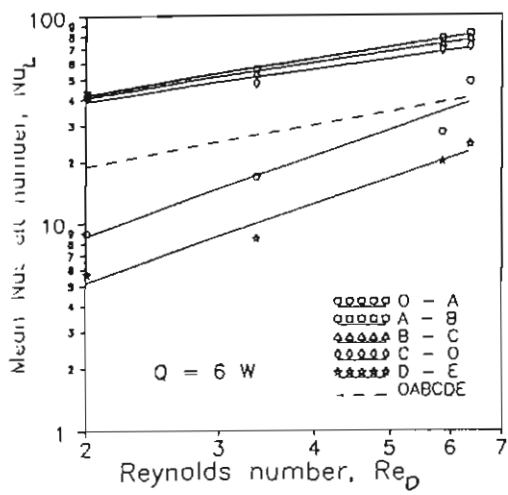


Fig. 4 Variation of average Nusselt number along the downstream and upstream base plate sections OA and DE and the three surfaces of the heater AB, BC, and CD for Reynolds number values $20500 \leq Re \leq 63000$ and fixed heating values of $Q = 6, 22, 51$ and 70 W .

and 70W. For all values of generated power, and the whole range of Reynolds number, the maximum temperature occurs at the horizontal upper surface of the heater. With the increase of the generated power Q , the maximum temperature of the right heater face (C-D) becomes closer to the maximum temperature of the upper surface (BC). The maximum temperature of the heater which occurs at the upper horizontal surface can be correlated by both Reynolds number and heat generated power by the following relations:

$$\begin{aligned} T_{\max} &= 2694.97 \text{ Re}^{-0.3646} && \text{for } Q = 70 \text{ W} \\ T_{\max} &= 1814.59 \text{ Re}^{-0.346} && \text{for } Q = 51 \text{ W} \\ T_{\max} &= 1283.69 \text{ Re}^{-0.3766} && \text{for } Q = 22 \text{ W} \\ T_{\max} &= 176.71 \text{ Re}^{-0.2125} && \text{for } Q = 6 \text{ W} \end{aligned}$$

Figure 4 shows the variation of average Nusselt number along the downstream and upstream base plate sections OA and DE as well as the three surfaces of the heater AB, BC, and CD for Reynolds number values $20500 \leq \text{Re} \leq 63700$ and fixed heating values of $Q = 6, 22, 51$ and 70W . For all values of the heat generated, and the whole range of Reynolds number, the maximum value of the average Nusselt number occurs at the left vertical surface (A-B) which faces the colder inlet air flow then followed by the horizontal and the right surfaced of the heater respectively. The base conductive plate, which absorbs part of the generated heat in the heat source, less values of Nusselt number than those of any of the generating heater surfaces. The upstream part of the conductive plate OA, which is met by the cold air flow, has higher values of the average Nusselt number than those of the downstream part of the base plate DE.

The variation of the average Nusselt number along the five surfaces of the base plate and the heater surfaces with Reynolds number is shown in Fig. 4 by the dashed lines. It can be correlated to Reynolds number for fixed heating values of heat generated by the following relations:

$$\begin{aligned} \bar{Nu} &= 0.375 \text{ Re}^{0.583} && \text{for } Q = 70 \text{ W} \\ \bar{Nu} &= 0.381 \text{ Re}^{0.571} && \text{for } Q = 51 \text{ W} \\ \bar{Nu} &= 0.220 \text{ Re}^{0.625} && \text{for } Q = 22 \text{ W} \\ \bar{Nu} &= 0.131 \text{ Re}^{0.654} && \text{for } Q = 6 \text{ W} \end{aligned}$$

Flow Visualization Patterns:

Beside the heat transfer experiments, flow visualization was performed using the oil-lampblack technique [16]. To get these visualization experiments, the surface of heating element with its base was covered with aluminum foil before the mixture of oil and lampblack powder was applied. When the air flow in the wind tunnel was initiated and maintained, the aerodynamic forces acting on the heating element and its base caused the mixture to move and take a pattern indicative of the pattern of fluid flow adjacent to the surface. To obtain a record of the visualization pattern, the aluminum foil was removed from the three heating element surfaces and its base plate, laid flat, and photographed. The results shown in Fig. 5, presents pattern of streaks which reveal the flow path of the air on the five different surfaces at Reynolds numbers from 20500 to 63700. The separation of the flow occurs on the surfaces of the heater A-B, B-C, AND C-D, and increases with the increase of Reynolds number. It is shown also that,

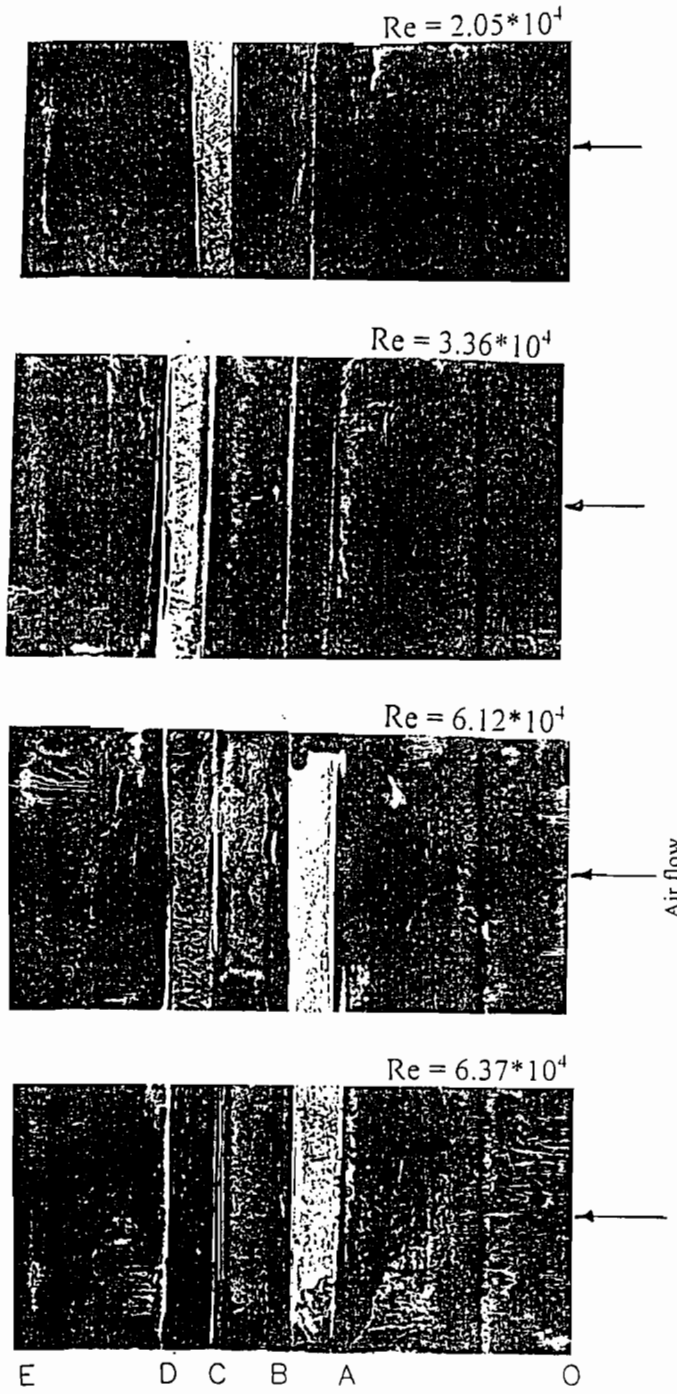


Fig. 5 Flow visualization pattern along the downstream and upstream base plate sections OA, DE and the three surfaces of the heater AB, BC, and CD for Reynolds number values $20500 \leq Re \leq 63000$.

at low values of Reynolds number, no strikes are noticed on the upstream surface of the base plate O-A, while, with the increased of Reynolds number, the strike pattern is noticed and its intensity is strongly increased. On the downstream plate surface, It is also noticed that, with the increase of Reynolds number, the strike pattern intensity increases also, but with lower rates than it on the upstream base plate surface.

CONCLUSION

Experimental results were obtained for the forced convection from a single protruding heat source, which is attached on a conductive plate. The range of air flow velocity is from 2.56 to 7.96 m/s which gives range of Reynolds number from 20500 to 63700. The power generated from the heat source was varied from 6 to 70W. The effect of Reynolds number, the generated heat power from the heater on the local and maximum surface temperatures and the average Nusselt number were presented, and the following conclusions were obtained:

The temperature at the base plate decreases suddenly in the downstream and upstream regions adjacent to the heater vertical surfaces. In the rest of the base plate the temperature decreases with lower rates as the distance from the heater increases. With the increase of the base plate length, it absorbs more heat from the heat source, which in turn decreases the level of the local heater surface temperatures. With the increase of Reynolds number the local surface temperatures of the heater and base plate decrease.

The maximum temperature occurs at the horizontal upper surface of the heater. With the increase of the generated power, the maximum temperature of the downstream vertical heater face becomes closer to the maximum temperature of the upper surface.

The maximum value of the average Nusselt number occurs at the upstream vertical surface and is followed by the horizontal then by the vertical downstream surfaces of the heater, respectively. The base conductive plate has less values of Nusselt number than that of any of the generating heater surfaces. The upstream part of the conductive plate has higher values of average Nusselt number than that of the downstream part.

The maximum temperature and the average Nusselt number along the five surfaces of the base plate and the heater surfaces is correlated with Reynolds number for fixed values of heat generated power by power relations:

$$T_{\max} = a Re^b, \quad \bar{Nu} = c Re^d$$

Where, a, b, c, and d are constants depends on the generated power.

V. NOMENCLATURE

| | | | |
|-----------------|---|-----------------|--|
| D | Channel hydraulic diameter, m | Q | Generated heat from the heater surface, W |
| k | Air thermal conductivity, W/mK | Re _D | Reynolds number, $Re = u_m D / \nu$ |
| L | Heater length, m | T | Temperature, C |
| Nu _L | Local Nusselt number along the heater surface | T ₀ | Inlet air temperature, C |
| \bar{Nu}_L | Average Nusselt number | u ₀ | Free air velocity, m/s |
| Pr | Prandtl number, ν/α | α | Air thermal diffusivity, m ² /s |
| q | heat flux from the heater surface, W/m ² | ν | Air kinematic viscosity, m ² /s |

VI. REFERENCES

1. Jaluria, Y., "Natural Convective Cooling of Electronic Equipment," in "Natural convection, Fundamentals & Applications" Kakac, S., Aung, V., and Viskanta, R., Hemisphere Publishing corporation, pp. 961-986, 1985.
2. Incropera, F. P., "Convection Heat Transfer in Electronic Equipment Cooling," ASME J. of Heat Transfer, Vol. 110, pp. 1097-1111, 1988.
3. Papanicolaou, E., and Jaluria, Y., "Mixed Convection From Simulated Electronic Components at Varying Relative Positions in a Cavity," ASME J. of Heat Transfer, Vol. 116, pp. 960-970, 1994.
4. El Kady, M. S., and Araid, F. F., "Natural Convection From a Single Surface Heater in a Vertical Rectangular Enclosure," Mansoura Engineering Journal (MEJ), Vol. 23, No. 2, pp. M -M , June, 1998.
5. Ramadhyani S., Moffatt D. F., and Incropera F. P., "Conjugate Heat Transfer from Small Isothermal Heat Sources Embedded in a Large Substrate," Int. J. Heat Mass Transfer, Vol. 28, No. 10, pp. 1945-1952, 1985.
6. Incropera, F. P., Kerby, J. S., Moffatt, D. F., and Ramadhyani, S., "Conjugate Heat Transfer from Discrete Heat Sources in a Rectangular Channel," Int. J. Heat Mass Transfer, Vol. 29, No. 7, pp. 1051-1058, 1986.
7. Davalath J., and Bayazitoglu, Y., "Forced Convection Cooling Across Rectangular Blocks," ASME J. of Heat Transfer, Vol. 109, pp. 321-328, 1987.
8. Wadsworth D. C., and Mudawar I., "Cooling of a Multichip Electronic Module by Means of Confined Two-dimensional jets of Dielectric Liquid," ASME J. of Heat Transfer, Vol. 112, pp. 891-898, 1990.
9. Kim S. K., and Anand N. K., "Laminar Developing Flow and Heat Transfer Between a Series of Parallel Plates with Surface Mounted Discrete Heat Sources," Int. J. Heat Mass Transfer, Vol. 37, No. 15, pp. 2231-2244, 1994.
10. Kim S. K., and Anand N. K., "Turbulent Heat Transfer Between a Series of Parallel Plates With Surface-Mounted Discrete Heat Sources," ASME J. of Heat Transfer, Vol. 116, pp. 577-587, 1994.
11. Molki, M., Faghri, M., and Ozbay, O., "Correlation for Heat Transfer and Weight Effect in the Entrance Region of an Inline Array of Rectangular Blocks Simulating Electronic Components," ASME J. of Heat Transfer, Vol. 117, pp. 40-46, 1995.
12. Hwang J., and Liou T., "Heat Transfer and Friction in a Low Aspect Ratio Rectangular Channel with Staggered Perforated Ribs on Two Opposite Walls," ASME J. of Heat Transfer, Vol. 117, pp. 843-850, 1995.
13. Nakayama, W., and Park, S. H., "Conjugate Heat Transfer From a Single Surface-Mounted Block to Forced Convective Air Flow in a Channel," ASME J. of Heat Transfer, Vol. 118, pp. 301-308, 1996.
14. Fowler A. J., Ledezma G. A., and Bejan A., "Optimum Geometric Arrangement of Staggered Plates in Forced Convection," Int. J. Heat Mass Transfer, Vol. 40, No. 18, pp. 1795-1805, 1997.
15. Incropera, F. P., Kerby, J. S., Moffatt, D. F., and Ramadhyani, S., "Convection Heat Transfer from Discrete Heat Sources in a Rectangular Channel," Int. J. Heat Mass Transfer, Vol. 29, No. 7, pp. 1051-1058, 1986.
16. Shalaby, M. A., and Araid, F. F., "Heat Transfer and Flow Visualization of Separated Reattached Air Flow Over Reversed Rectangular Flat Plate," MEJ, Vol. 12, No. 1, June 1987.